Supporting Information

Observation of Fullerene Soot in Eastern China

Junfeng Wang,[†] Timothy B. Onasch,[‡] Xinlei Ge,[†,*] Sonya Collier,[§] Qi Zhang,[§,†]

Yele Sun,[‖] Huan Yu,[†] Mindong Chen, [†,*] André S.H. Prévôt,[⊥,†,#] Douglas R.Worsnop[‡]

[†]Jiangsu Key Laboratory of Atmospheric Environment Monitoring and Pollution Control(AEMPC), Collaborative Innovation Center of Atmospheric Environment and Equipment Technology (AEET), School of Environmental Science and Engineering, Nanjing University of Information Science & Technology, Nanjing 210044, China

[‡]Aerodyne Research Inc., Billerica, MA 01821, United States

[§]Department of Environmental Toxicology, University of California at Davis, Davis, CA 95616, United States

[‖]State Key Laboratory of Atmospheric Boundary Layer Physics and Atmospheric Chemistry, Institute of Atmospheric Physics, Chinese Academy of Sciences, Beijing 100029, China

[⊥]Laboratory of Atmospheric Chemistry, Paul Scherrer Institute, Villigen 5232, Switzerland

[#]Key Laboratory of Aerosol Chemistry and Physics, Institute of Earth Environment, Chinese Academy of Sciences, Xi'an710075, China

Corresponding Author, *Email: caxinra@163.com; chenmdnuist@163.com

Phone: +86-25-58731394

Sampling site, instrument operations and calibrations

The Aerodyne Soot Particle Aerosol Mass Spectrometer (SP-AMS) was deployed during February 20- March 23, 2015. The SP-AMS was housed in the Observatory Lab inXueke No.1 Building (32°12′20.82″N, 118°42′25.46″E), Campus of Nanjing University of Information Science and Technology (NUIST) in suburban Nanjing, located onthe north side of the Yangtze River. The sampling site was located west/southwest of an industrial zone with a large number of petrochemical and chemical plantsand a densely populated residential area (Figure S1). There are also many diesel trucks frequently passing by the arterial roads within a 2km radius to the sampling site with no restrictions. During measurement, ambient air was drawn through a 16.7L min^{-1}, 1μm cyclone (URG-2000-30EHB, URG Corp., Chapel Hill, NC) (~5m above the ground), but the gas flow rate was adjusted to ~5L/min to achieve a size cut of ~2.5 μm based on the cyclone's efficiency curve. The sampled air then passed through a diffusions dryer filled with silica gel (replaced/regenerated twice during the campaign) to remove moisture and maintain a relative humidity level below 12% before entering into the SP-AMS. The sampling line was in total roughly 3 m long assembled using ¼ - ½ inch stainless steel or copper tubing and proper fittings.

The SP-AMS was carefully tuned including optimization of laser beam/particle beam alignment, instrument sensitivity and chemical resolution, etc. As the instrument has both thermal vaporizer and laser vaporizer, it was operated in a cycle consisting of six modes/menu settings (M1: Laser on V-mode; M2: Laser off V-mode; M3: Laser on W-mode; M4: Laser off W-mode; M7: Laser on PToF-mode; M8: Laser off PToF-mode) (note the thermal vaporizer was always turned on and kept around 600 ^{o}C), with each mode lasting 2.5 min adding up to a total cycle of 15 min. The V- and PToF-modes (under V-mode but with chopper running on ~2% duty cycle) have better sensitivity for mass quantification, while the W-mode has enhanced chemical resolution. The *m/z* range for M1 and M2, M7 and M8 and M3 and M4 was ~2000for fullerene soot measurement, ~1000 specifically for particle size measurement and ~450, for improved separation of small *m/z* ions, respectively. In order to determine the instrument detection limits for the measured aerosol species, two filtered ambient air tests were conducted on March 11 (11am - 1pm) and March 23 (10am – 1pm), 2015.

The instrument was calibrated for mass quantification, e.g., ionization efficiency (IE), using size-selected monodisperse pure ammonium nitrate particles following the procedures described in Jayne et al. [1]Different concentrations of aqueous solutions of NH_4NO_3were nebulized to generate particles, which were dried and size-selected (250 nm and 300 nm) using a Scanning Mobility Particle Sizer (SMPS, TSI Inc., Shoreview, MN, USA) before entering into the SP-AMS.Relative ionization efficiency (RIE) ofammonium wasalso determined, and RIE of sulfate was calibrated using pure ammonium sulfate separately. The RIE*s* for nitrate, sulfate, chloride, ammonium and organics were 1.05, 1.18, 1.3, 2.99 and 1.4, respectively.

For *r*BC (non-fullerene ions, C_1^+-C_{31}^+), with both thermal and laser vaporizers on, we determined its RIE by using Regal Black (REGAL 400R pigment black, Cabot Corp.) as the calibration material,[2] and its RIE was determined to be 0.2.Since a series of fullerene soot-like (FS-like) ions (C_{32}^+-C_{160}^+) were observed, and they showed a very similar spectral pattern as the fullerene soot standard (Alfa Aesar, stock# 40971, lot# E23Q17, AAFS standard), we performed additional calibrations on the FS-like ions using the AAFS standard following the similar procedure for *r*BC(C_1^+-C_{31}^+) calibration. Since Regal Black and AAFS standard particles are water-insoluble, their solutions were atomized under sonication to maintain relatively stable aerosol concentrations. Particularly, for the mass calibration of FS-like ions, (1) we used the effective densities reported by Gysel et al.[3] to calculate the mass of monodisperse AAFS standard particles delivered into the SMPS; (2) since the M7 setting which measures the size distributions of the AAFS standard particles can only measure the *m/z* up to ~1000, the masses of the FS-like ions (C_{32}^+-C_{160}^+) were scaled according to the mass fraction of <1000 fullerene ions to its standard full mass spectrum; (3) we considered that the content of fullerenes in the AAFS standard is 7.2 wt%. Finally, we derived a RIE for the FS-like ions of 5.0.

Size calibration was performed by using the standard polystyrene latex (PSL) spheres (Duke Scientific Corp., Palo Alto, CA) with sizes across 100 – 700 nm range in the middle of the campaign, following the procedures detailed in Canagaratna et al.[4]

Calibrations on ammonium nitrate, ammonium sulfate, *r*BC (C_1^+-C_{31}^+) were conducted in the beginning, middle and end of the campaign, while the FS-like ions calibration was conducted in the middle and end of the study as we didn't anticipate their

occurrence prior to the measurement.

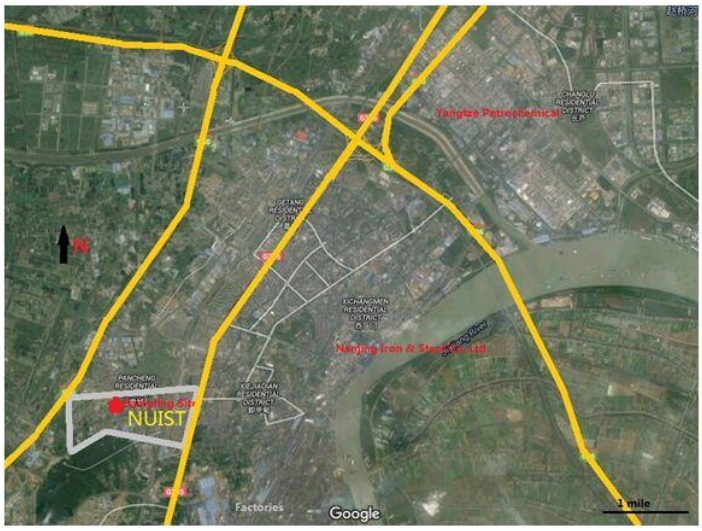

Figure S1. The sampling site and its surroundings (Image was created based on Google Map: https://www.google.com/permissions/geoguidelines/attr-guide.html)

Identification and mass calculation of FS-like ions

As the FS-like ions have large *m/z* values, the ion separating ability is significantly decreased as the V-mode mass resolution is 2000 ~ 3000, the SP-AMS is still able to unambiguously identify and confirm the occurrence of FS-like ions, based on the following reasons.

(1) The presence of organic ions with similar masses as fullerenes is highly unlikely (in particularly for ones >*m/z* 600). For example, as shown in Figure S8, there are only noises at ~*m/z* 720 when the laser is off; when the laser is on, significant peaks occur, indicating these peaks can only be vaporized by the laser, referring to refractory BC components in a traditional sense. In addition, if such large *m/z* species do present in an appreciable amount in ambient particles, they might be observed by other types of AMS, yet such species had never been reported.

(2) As mentioned in the main text, another strong evidence for *m/z* 720 to be C_{60}^+, is that the signal intensity ratios between the 4 *m/z*s (720, 721, 722, 723) (in Figure 1 of the main text) match exactly the isotopic ratios of the C_{60} reference spectrum in the NIST database. This should be true for C_{70} cluster and other fullerene ions as every fullerene carbon cluster observed contains such 4 isotopic ions, and there are no other significant

peaks are seen besides them.

(3) The signals at *m/z* 720 and *m/z* 840 clearly stand out as "magic number" in the ion series, indicating the stable fullerene structures.[5] Moreover, dominant carbon ions are spaced at 24 amu (i.e., two carbon atoms), with much weaker peaks spaced at 12 amu (i.e., one carbon atom), in accordance with the hollow-3D or closed structure and reactivity of fullerenes.[6]

(4) Previously, 12 types of different *r*BC particles produced by industrial and combustion processes were measured using the SP-AMS, in order to explore the distributions of the carbon ions obtained by the SP-AMS for different *r*BC materials.[7] Their mass spectra were acquired under the similar conditions as we did during the field campaign presented in this work. Overall, we found that only the *r*BC materials with high content of fullerenes can yield significant fullerene ion signals**.** Thus, the occurrence of FS-like ion signals must indicate the presence of fullerene-related species. That said, by using the SP-AMS, we do measure fullerene ion signals when expected (in fullerene soot/black and C_{60}), and not where no fullerenes are expected (in graphitic and amorphous carbon).

For the mass calculation of the FS-like ions, we used the "UMR method" rather than the HR fitting. The HR fitting aims to apportion the total signal to different ions via a multi-peak fitting algorithm. As most ions are less than 200 amu, the HR fitting parameters, including peak shape and peak width, are determined based on selected small *m/z* ions. Note the signal of small *m/z*s is typically distributed within $\pm$0.15 amu around the integer *m/z* (such as 60-63 in Figure S2), yet the distribution pattern for the FS-like ions (such as 720-723) is very different – their peaks have large tails and can distribute over the full m/z. This feature means that the HR fitting parameters cannot accurately account for the signals of FS-like ions. On the other hand, the UMR method integrates all signals under the curve of a certain *m/z* as the amount of that *m/z*. Note the baseline parameters such as the stick region, should also be carefully modified in order to account for all signals. Clearly, in this case, the UMR method is more accurate than the HR method. For the AAFS standard, we used the exactly same approach, thus the quantification is consistent.

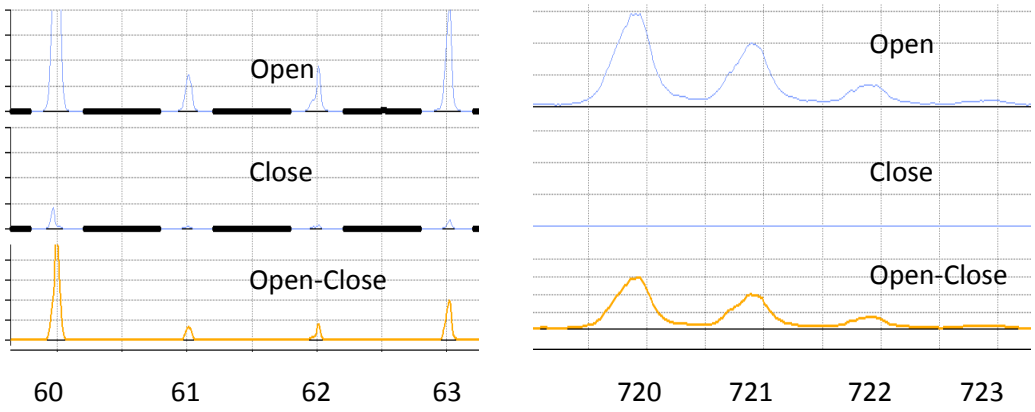

Figure S2. Examples of the signal distribution pattern of small (60-63) and large *m/zs* (720-723)

Positive Matrix Factorization (PMF) analyses

The PMF analyses were conducted on the organic aerosol (OA) spectra (obtained under W mode with laser on, e.g., M3 setting) according to the principles outlined in Zhang et al.[8] The analysis included ions with *m/z* up to 120 in this work. Six-factor solution was chosen as the optimal solution, with corresponding factor profiles, time series and diurnal variations shown in Figure S3. The six factors include three primary OA factors, hydrocarbon-like OA (HOA) that often relates with traffic activities, cooking-related OA (COA), industry-related OA (IOA), and three secondary OA factors, e.g., a semi-volatile oxygenated OA (SVOOA), a low-volatility oxygenated OA (LVOOA), and a specific local secondary OA (LSOA). The HOA is abundant in hydrocarbon ions, and the COA has significant oxygenated ions at *m/z* = 55 and *m/z* = 57; these spectral features and their diurnal patterns are both similar to ones identified in other locations.[9] A specific IOA was separated in this study: this factor has a relative high fraction of CO_2^+, and its temporal variations behave very differently from HOA (r^2= 0.03) and COA (r^2 = 0.01) (although the diurnal trend of IOA is somewhat similar to that of HOA). The SVOOA and LVOOA also have similar features with those identified by the AMS community:[10] SVOOA has a smaller $CO_2^+/C_2H_3O^+$ ratio while LVOOA has a larger $CO_2^+/C_2H_3O^+$ ratio; SVOOA correlates better with nitrate (r^2= 0.53) than with sulfate (r^2= 0.31) while LVOOA correlates better with sulfate (r^2= 0.46) than with nitrate (r^2= 0.26). In addition, an LSOA factor was also identified, accounting for relatively

smaller mass fraction (10%) of the total OA than other factors.

For comparison, in the case of 5-factor solution (Figure S4), factor 4 (likely COA) has a high oxygen-to-carbon ratio of 0.31, and factor 1 and factor 2 (the two OOA factors) have the same O/C ratios of 0.46, and the correlation coefficient of factor 1 (likely SVOOA) with nitrate (r^2= 0.35) is much worse than that of the SVOOA from the 6-factor solution with nitrate (r^2= 0.53), all indicating the mixing effects of factor 1 (SVOOA) and factor 4 (COA). The 7-factor solution (Figure S5), on the other hand, clearly split the LVOOA factor into two OOA factors (factor 2 and factor 3) while retaining the basic characteristics of the other four factors.

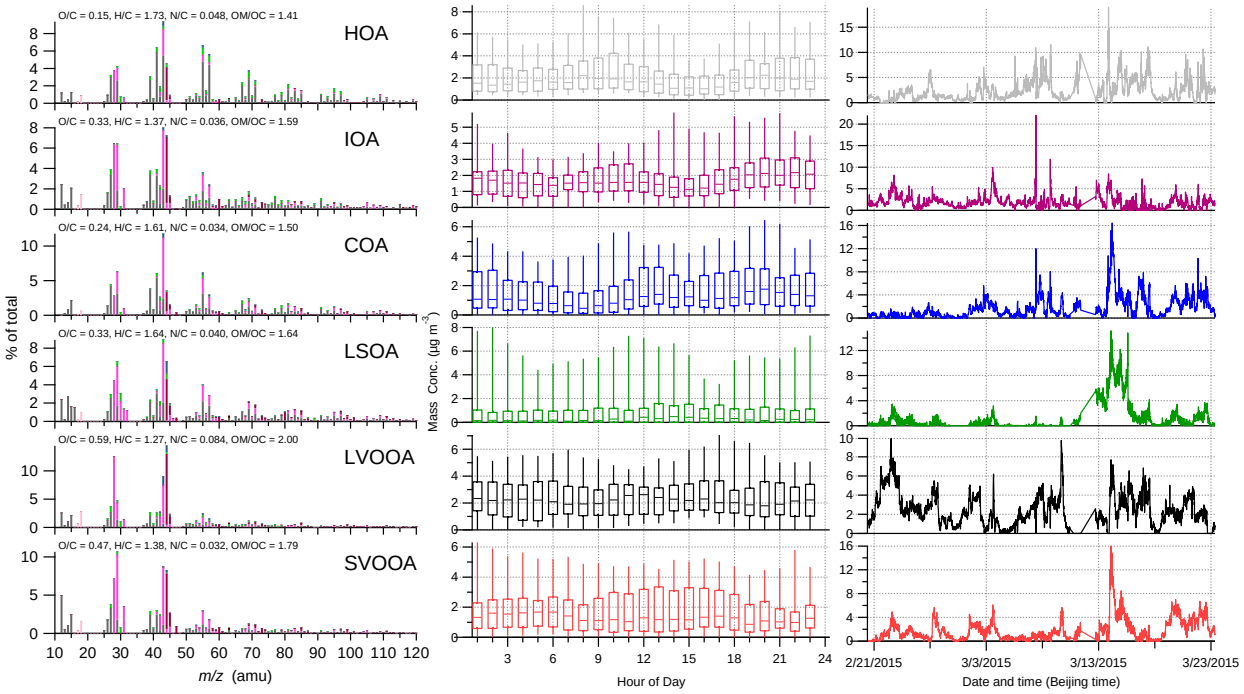

Figure S3.Mass spectra (left panel), diurnal patterns (middle panel) and time series (right panel) of the PMF factors (optimal 6-factor solution).

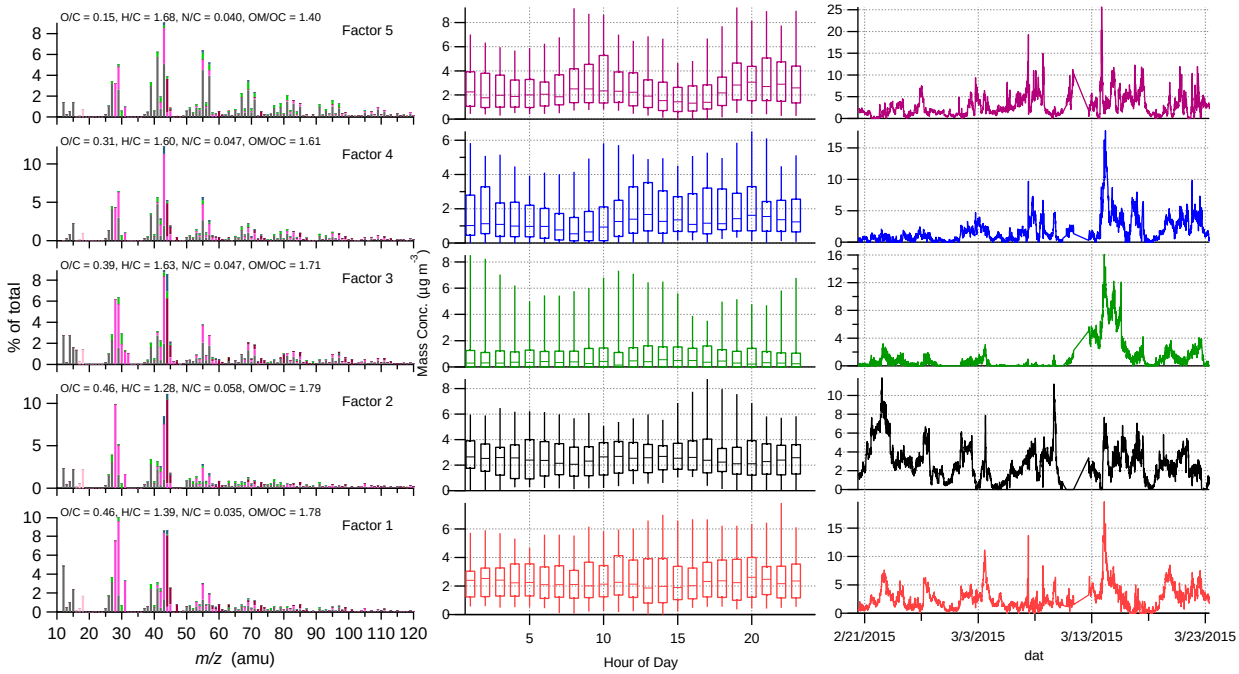

Figure S4. Mass spectra (left panel), diurnal patterns (middle panel) and time series (right panel) of the PMF 5-factor solution.

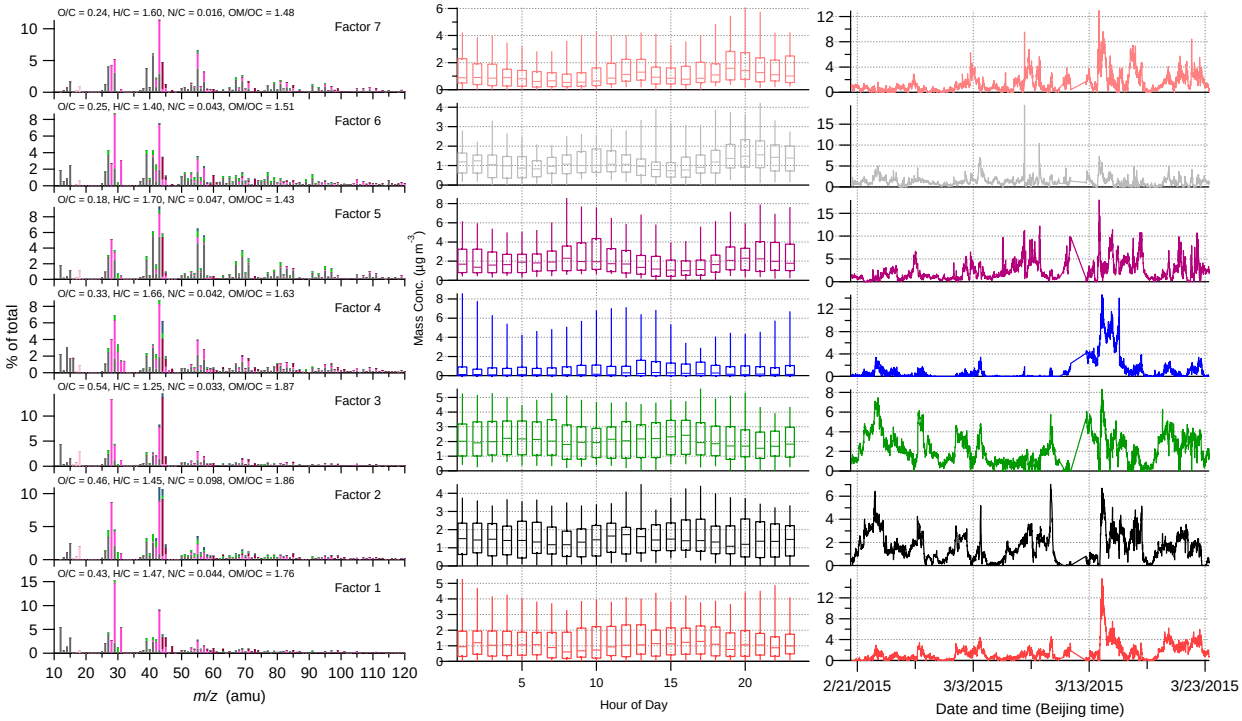

Figure S5. Mass spectra (left panel), diurnal patterns (middle panel) and time series (right panel) of the PMF 7-factor solution.

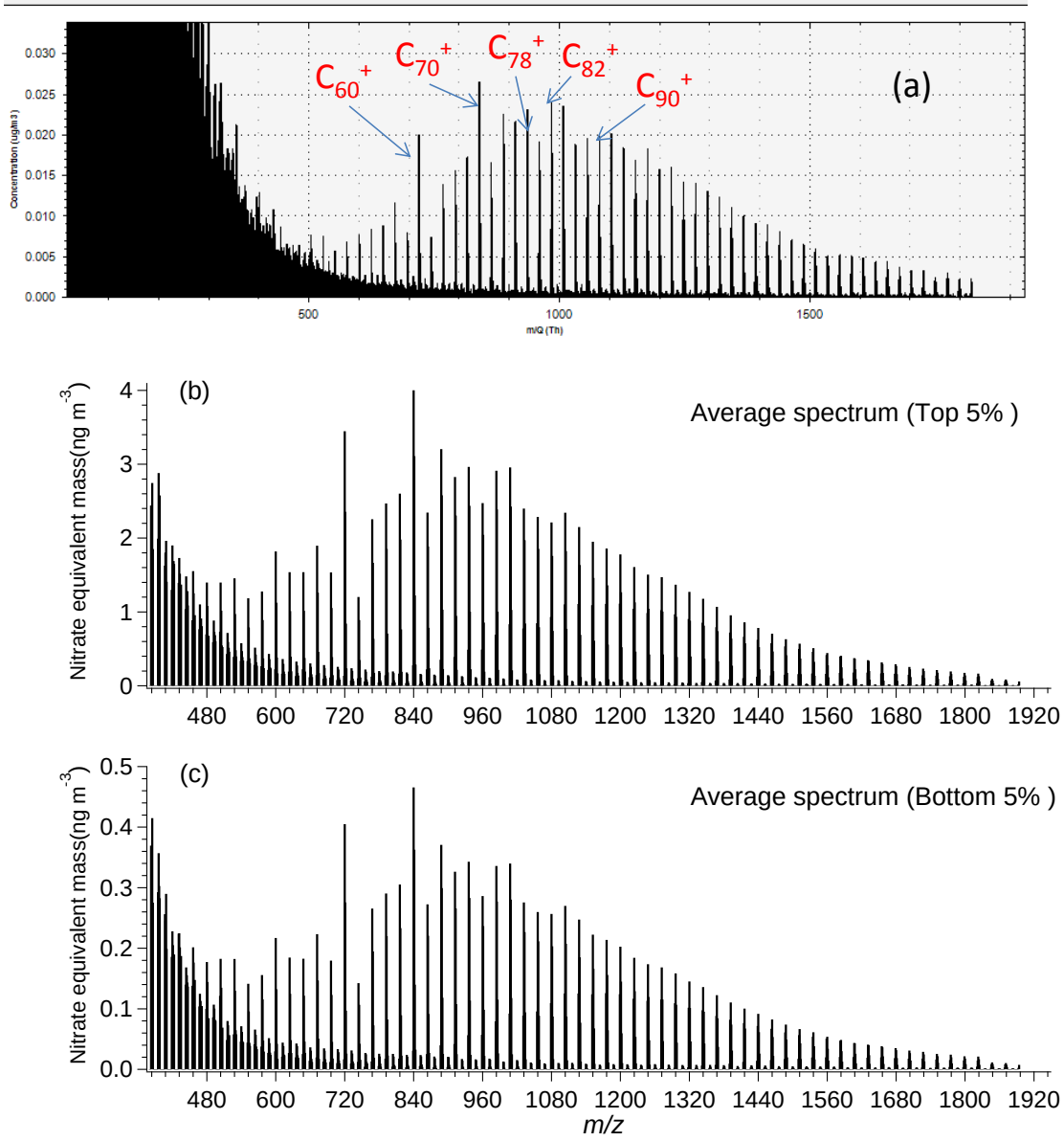

Figure S6. (a) A screenshot of the real-time display of FS-like ions during measurement (concentrations displayed are not calibrated), and the average mass spectra for these FS-like ions with concentrations of top 5% (b) and bottom 5% (c).

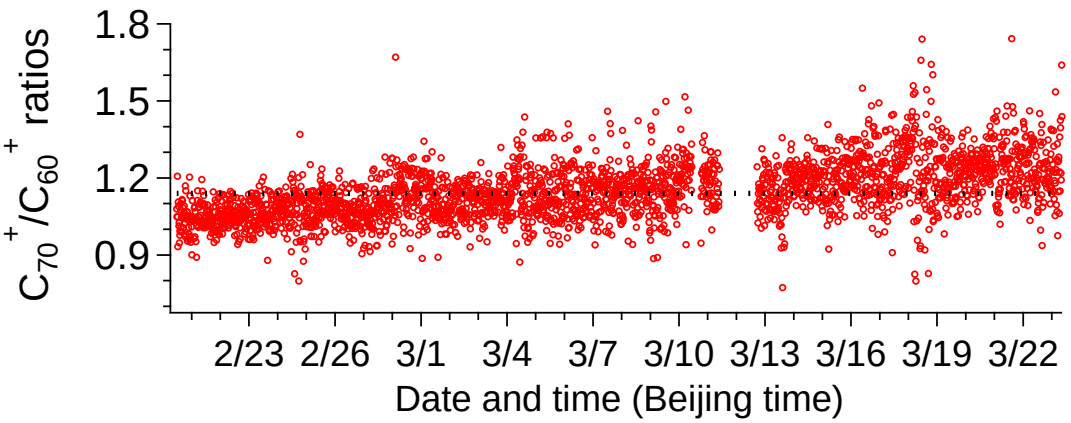

Figure S7. Measured C_{70}^{+}/C_{60}^{+} ratios across the sampling period.

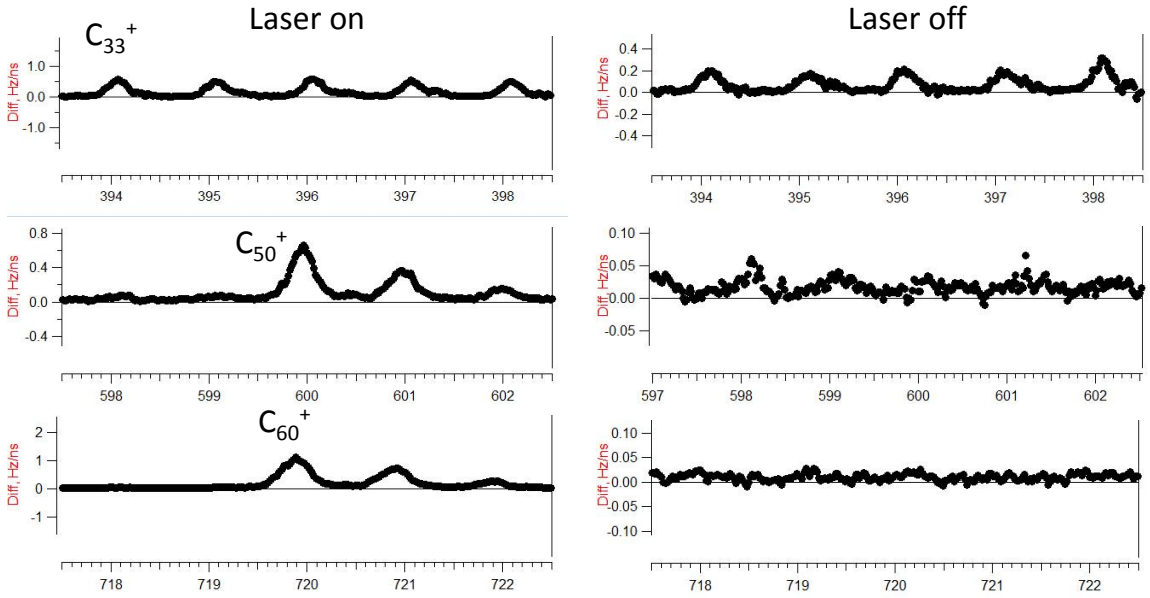

Figure S8. Examples of the spectral signals with laser on (left panel) and laser off (right panel) of ambient particles around C_{33}^{+} (*m/z* = 396), C_{50}^{+} (*m/z* = 600) and C_{60}^{+} (*m/z* = 720). Significant signals exist at C_{33}^{+}-related ions even when the laser was off, indicating influences from non-fullerene organics; while interference from non-fullerene signals on C_{50}^{+}- and C_{60}^{+}-related ions is negligible when the laser was off.

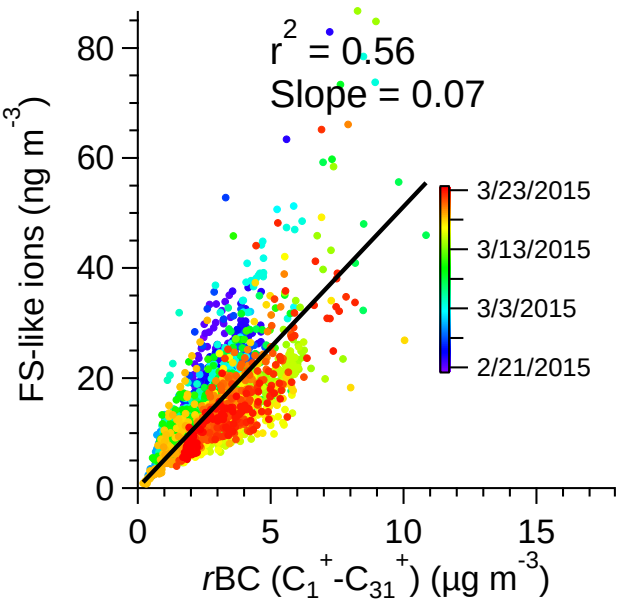

Figure S9. Scatter plots and linear fits between mass concentrations of FS-like ions with *r*BC (C_1^+-C_{31}^+).

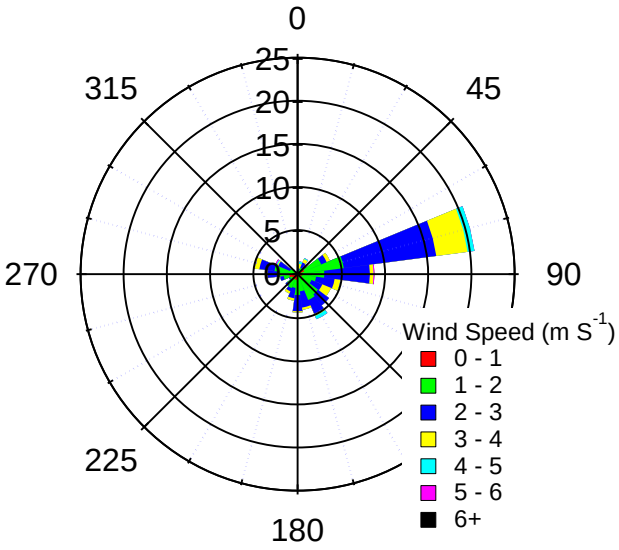

Figure S10. Wind rose plot for the entire campaign.

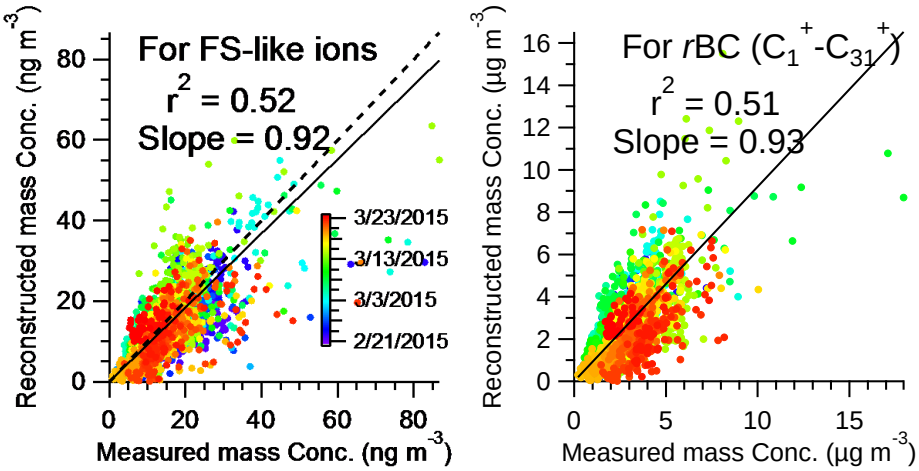

Figure S11. Scatter plots and linear fits between the reconstructed and measured FS-like ions (a), and the reconstructed and measured *r*BC(C_1^+-C_{31}^+) (b). Data points are colored by time.

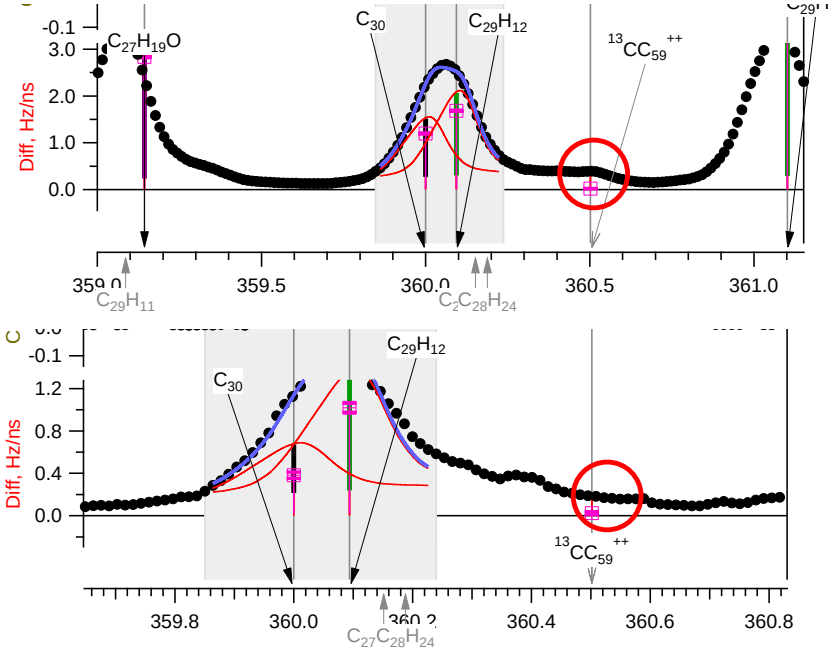

Figure S12. Examples of the spectral signals with laser on (top panel) and laser off (bottom panel) of ambient particles around $^{13}CC_{59}^{2+}$ (*m/z* = 360.5, red circle). Relatively clear peak can be observed in the mass spectrum with laser on.

Table S1. Correlation coefficients (r^2) for the time-dependent mass concentrations for the fullerene soot and *r*BC (C_1^+-C_{31}^+) with other aerosol components.

r^2	Nitrate	Sulfate	Chloride	HOA	IOA	COA	LSOA	SVOOA	LVOOA
FS-like ions	0.08	0.15	0.07	0.12	**0.45**	0.06	0.07	0.07	0.06
*r*BC (C_1^+-C_{31}^+)	0.32	0.26	0.23	**0.36**	0.22	0.30	0.29	0.24	0.10

References

1. Jayne, J. T.; Leard, D. C.; Zhang, X.; Davidovits, P.; Smith, K. A.; Kolb, C. E.; Worsnop, D. R., Development of an Aerosol Mass Spectrometer for Size and Composition Analysis of Submicron Particles. *Aerosol Sci. Tech.* **2000,** *33* (1), 49 - 70.
2. Onasch, T. B.; Trimborn, A.; Fortner, E. C.; Jayne, J. T.; Kok, G. L.; Williams, L. R.; Davidovits, P.; Worsnop, D. R., Soot Particle Aerosol Mass Spectrometer: Development, Validation, and Initial Application. *Aerosol Sci. Tech.* **2012,** *46* (7), 804-817.
3. Gysel, M.; Laborde, M.; Olfert, J. S.; Subramanian, R.; Grohn, A. J., Effective Density of Aquadag and Fullerene Soot Black Carbon Reference Materials Used for Sp2 Calibration. *Atmos. Meas.Tech.* **2011,** *4* (12), 2851-2858.
4. Canagaratna, M. R.; Jayne, J. T.; Jimenez, J. L.; Allan, J. D.; Alfarra, M. R.; Zhang, Q.; Onasch, T. B.; Drewnick, F.; Coe, H.; Middlebrook, A. et al., Chemical and Microphysical Characterization of Ambient Aerosols with the Aerodyne Aerosol Mass Spectrometer. *Mass Spectrom. Rev.* **2007,** *26* (2), 185-222.
5. Fowler, P. W., How Unusual Is C60? Magic Numbers for Carbon Clusters. *Chemical Physics Letters* **1986,** *131* (6), 444-450.
6. Bowers, M. T., Ion Mobility Spectrometry: A Personal View of Its Development at Ucsb. *Int. J. Mass Spectrom.* **2014,** *370*, 75-95.
7. Onasch, T. B.; Fortner, E. C.; Trimborn, A. M.; Lambe, A. T.; Tiwari, A. J.; Marr, L. C.; Corbin, J. C.; Mensah, A. A.; Williams, L. R.; Davidovits, P. et al., Investigations of Sp-Ams Carbon Ion Distributions as a Function of Refractory Black Carbon Particle Type. *Aerosol Sci. Tech.* **2015,** *49* (6), 409-422.
8. Zhang, Q.; Jimenez, J.; Canagaratna, M.; Ulbrich, I.; Ng, N.; Worsnop, D.; Sun, Y., Understanding Atmospheric Organic Aerosols Via Factor Analysis of Aerosol Mass Spectrometry: A Review. *Anal. Bioanal. Chem.* **2011,** *401* (10), 3045-3067.
9. Ge, X. L.; Setyan, A.; Sun, Y.; Zhang, Q., Primary and Secondary Organic Aerosols in Fresno, California During Wintertime: Results from High Resolution Aerosol Mass Spectrometry. *J. Geophys. Res. - Atmos.* **2012,** *117* (D19), D19301.
10. Xu, J.; Zhang, Q.; Chen, M.; Ge, X.; Ren, J.; Qin, D., Chemical Composition, Sources, and Processes of Urban Aerosols During Summertime in Northwest China: Insights from High-Resolution Aerosol Mass Spectrometry. *Atmos. Chem. Phys.* **2014,** *14* (23), 12593-12611.